

# Spectral-based 2D/3D X-ray to CT image rigid registration

M. Freiman<sup>a</sup>, O. Pele<sup>a</sup>, A. Hurvitz<sup>a</sup>, M. Werman<sup>a</sup>, L. Joskowicz<sup>a</sup>

<sup>a</sup>School of Engineering and Computer Science, The Hebrew University of Jerusalem, Israel.

## ABSTRACT

We present a spectral-based method for the 2D/3D rigid registration of X-ray images to a CT scan. The method uses a Fourier-based representation to decompose the six rigid transformation parameters problem into a two-parameter out-of-plane rotation and a four-parameter in-plane transformation problems. Preoperatively, a set of Digitally Reconstructed Radiographs (DRRs) are generated offline from the CT in the expected in-plane location ranges of the fluoroscopic X-ray imaging devices. Each DRR is transformed into an imaging device in-plane invariant features space. Intraoperatively, a few 2D projections of the patient anatomy are acquired with an X-ray imaging device. Each projection is transformed into its in-plane invariant representation. The out-of-plane parameters are first computed by maximization of the Normalized Cross-Correlation between the invariant representations of the DRRs and the X-ray images. Then, the in-plane parameters are computed with the phase correlation method based on the Fourier-Mellin transform. Experimental results on publicly available data sets show that our method can robustly estimate the out-of-plane parameters with accuracy of  $1.5^\circ$  in less than 1sec for out-of-plane rotations of  $10^\circ$  or more, and perform the entire registration in less than 10secs.

## 1. INTRODUCTION

The rigid registration of a preoperative CT to intraoperative X-ray fluoroscopic images has received considerable attention during the past decade, due to its relevance to Image-Guided Surgery (IGS) applications in orthopedics and interventional radiology. Compared to contact-based registration, it is often faster, more reliable, less prone to human error, and requires less operator training. It also allows for non-invasive and percutaneous procedures.

To use a preoperative CT intraoperatively for IGS, the CT must be registered to the physical patient in the operating room. In 2D/3D registration, the patient anatomy is imaged with a calibrated fluoroscopic X-ray C-arm from several viewpoints. The registration problem consists of finding the rigid transformation between these co-registered X-ray images and the CT.

Existing methods for 2D/3D rigid registration can be classified into three main groups: 1) feature-based methods; 2) intensity-based methods, and; 3) hybrid methods. For a recent review of these methods see.<sup>1</sup>

Feature-based methods<sup>2-4</sup> rely on the detection of corresponding geometric features in both the 3D CT volume and the 2D X-ray projections, and on finding the rigid transformation that minimizes the geometric distance between them. Extracting a few geometric features greatly reduces the amount of data, which results in fast registration in a wide convergence range. However, registration accuracy greatly depends on the accuracy of the features detection and the features matching. Consequently, feature-based methods are often less accurate and robust than alternative methods.

Intensity-based methods<sup>5-7</sup> search for the transformation that maximizes a similarity measure between image intensities. The CT volume is projected onto 2D images, called Digitally Reconstructed Radiographs (DRRs). The DRRs are compared directly to the X-ray images in the 2D domain using a similarity measure. Intensity-based methods are generally more accurate and robust than feature-based methods.<sup>8</sup> However, the DRR generation process makes intensity-based methods relatively slow.

Previous works address this drawback by offline DRR precomputation,<sup>6,9</sup> by restricting the matching to a region of interest, and/or by using multi-resolution schemes.<sup>6</sup> Further improvements are obtained with hardware acceleration methods.<sup>7</sup> A key drawback of intensity-based methods is their relatively small convergence range.

---

Further author information: (Send correspondence to M. Freiman)  
M. Freiman: E-mail: freiman@cs.huji.ac.il, Telephone: +1-617-355-2755

Hybrid methods<sup>10</sup> incorporate both geometric feature matching and intensity similarity metrics. For example, Tomazevic et al.<sup>11</sup> back-project the 2D information in the X-ray images into 3D and compute the CT to X-ray similarity metric in 3D. While these methods are more accurate than feature-based methods, they are computationally intensive due to the DRR generation.

All of the current DRR-based methods perform the optimization with an iterative search in the 6D space. The search requires a large number of iterations with costly computations to evaluate the image similarity at each iteration. In addition, the search may converge to local extrema. The decomposition of the search space can reduce the number of generated DRRs and speed up the search.

To accelerate the DRR computations, Cyr et al.<sup>12</sup> decompose the DRRs into C-arm imaging device in-plane and out-of-plane DRRs. However, the optimization is performed on the entire 6-dimensional search space, which tends to be slow. Fu et al.<sup>13</sup> propose to iteratively optimize first the in-plane parameters and then the out-of-plane parameters until convergence. The main drawback is that the in-plane optimization does not take into account local extrema due to missed out-of-plane parameters, which can result in non-optimal transformations. Dong et al.<sup>14</sup> describe an in-plane rotation invariant similarity measure based on Zernike moments, whose computation is expensive and whose results are sensitive to internal parameter settings.

In this paper we present a spectral-based approach for 2D/3D image rigid registration. Spectral-based phase-correlation 2D/2D image registration<sup>15,16</sup> has been shown to be robust to noise and intensity variations in illumination or radiation exposures thanks to the Fourier magnitude normalization. Spectral analysis provides a natural way to decompose the search space into in-plane and out-of-plane sub-spaces, which can be searched independently and guarantee global convergence. This yields a fast and robust rigid registration method with a relatively large convergence range: only a small number of DRRs are generated and stored, and only one DRR for each X-ray image is required intraoperatively to compute the in-plane parameters. The result is a very fast and memory-efficient method.

## 2. METHOD

Our 2D/3D rigid registration method consists of an offline preoperative and an online intraoperative phase. Preoperatively, a small set of out-of-plane DRRs are generated from the CT in the expected location ranges of the fluoroscopic X-ray C-arm imaging devices. The resulting DRRs are then transformed to Fourier-Mellin in-plane invariant features. Intraoperatively, for each X-ray image, its out-of-plane parameters are computed by cross-correlation with the preoperative DRRs. Then, the in-plane parameters are computed by generating a single DRR from the computed C-arm imaging device imaging plane and performing 2D/2D registration with the Fourier-Mellin method. The method requires the computation of two FFTs, one image transformation into the log-polar domain, and two phase correlations. Since the optimization of the out-of-plane and the in-plane parameters is done separately on a relatively small 2D grid, the global maximum is obtained in each stage, which ensures convergence to the global optimum. We describe each step in detail next.

### 2.1 Offline out-of-plane DRR generation

A set of DRRs is generated from the preoperative CT in the expected location ranges of the fluoroscopic X-ray C-arm imaging devices. The DRRs are generated for out-of-plane rotations about the two C-arm imaging device imaging plane axes. The sampling grid parameters are the rotations range; the difference between two samples can be set according to the desired accuracy and convergence range. Therefore, only a relatively small number of DRRs is required. For example, only 400 DRRs are required for a convergence range of  $-20^\circ$  to  $+20^\circ$  at  $2^\circ$  intervals.

### 2.2 Fourier-Mellin in-plane invariant features computation

The set of out-of-plane DRRs is transferred into a rotation, translation, and scale invariant representation based on the Fourier-Mellin transform.<sup>15</sup> We use the translational properties of the Fourier shift theorem (Eq. 2) to derive a representation of the 2D images that is invariant to in-plane rotation, translations, and scale using the magnitude spectrum.

Let  $F_1(\xi, \eta)$  and  $F_2(\xi, \eta)$  be the Fourier transforms of images  $f_1(x, y)$  and  $f_2(x, y)$  respectively. The in-plane invariant features generation consists of three steps: 1) Translations reduction, 2) Rotation reduction, and; 3) Scale reduction. We describe each step next.

**1. Translations reduction:** when  $f_2$  differs from  $f_1$  by a translation of  $(x_0, y_0)$ , we have:

$$f_2(x, y) = f_1(x - x_0, y - y_0) \quad (1)$$

using the Fourier shift theorem we get:

$$M_2 = |F_2(\xi, \eta)| = |e^{-j2\pi(\xi x_0 + \eta y_0)} \cdot F_1(\xi, \eta)| = |F_1(\xi, \eta)| = M_1 \quad (2)$$

Thus,  $M_1$  and  $M_2$  are translation invariant representations of the original images  $f_1$  and  $f_2$ .

**2. Rotation reduction:** when  $f_2$  differs from  $f_1$  by a translation of  $(x_0, y_0)$  as above and by an additional rotation of  $\theta_0$ , we have:

$$f_2(x, y) = f_1(x \cos \theta_0 + y \sin \theta_0 - x_0, -x \sin \theta_0 + y \cos \theta_0 - y_0) \quad (3)$$

using the Fourier translation and rotation properties,<sup>15</sup> we get:

$$F_2(\xi, \eta) = e^{-j2\pi(\xi x_0 + \eta y_0)} \cdot F_1(\xi \cos \theta_0 + \eta \sin \theta_0, -\xi \sin \theta_0 + \eta \cos \theta_0) \quad (4)$$

The magnitudes  $M_1$  and  $M_2$  of  $F_1$  and  $F_2$  are related by:

$$M_2(\xi, \eta) = M_1(\xi \cos \theta_0 + \eta \sin \theta_0, -\xi \sin \theta_0 + \eta \cos \theta_0) \quad (5)$$

The polar representation of  $M_1$  and  $M_2$  is:

$$M_2(\rho, \theta) = M_1(\rho, \theta - \theta_0) \quad (6)$$

where  $\rho$  and  $\theta$  are the radius and angle in the polar coordinate system, respectively. Thus,  $M_2$  and  $M_1$  are related by translation in their polar representation. Taking their Fourier magnitude (Eq. 2) yield a rotation and translation invariant representation.

**3. Scale reduction:** when  $f_2$  is a translated, rotated and scaled version of  $f_1$ , their corresponding Fourier magnitudes  $M_2$  and  $M_1$  are related by translations only in their log-polar representation:

$$M_2(\rho, \theta) = M_1(\rho/s, \theta - \theta_0) = M_2(\log \rho, \theta) = M_1(\log \rho - \log s, \theta - \theta_0) \quad (7)$$

where  $\rho$  and  $\theta$  are as before and  $s$  is the scale factor. Thus,  $M_2$  and  $M_1$  are related by translations in their log-polar representation and by taking their Fourier magnitude (Eq. 2), we obtain a translation, rotation, and scale and invariant representation.

### 2.3 Out-of-plane parameters computation

Each intraoperative fluoroscopic X-ray image of the patient anatomy is first transformed to its in-plane invariant representation as described in Section 2.2. Then, the out-of-plane rotation parameters are computed by searching for the precomputed DRR that maximizes the Normalized Cross-Correlation (NCC) of the in-plane invariant image representations:

$$(R_x, R_y) = \operatorname{argmax}_{r_x, r_y} \frac{\sum_{i=1}^n \sum_{j=1}^n \left( I_f(i, j) \cdot I_{d_{(r_x, r_y)}}(i, j) \right)}{\sqrt{\sum_{i=1}^n \sum_{j=1}^n I_f(i, j)^2 \cdot \sum_{i=1}^n \sum_{j=1}^n I_{d_{(r_x, r_y)}}(i, j)^2}} \quad (8)$$

where  $I_f$  is the fluoroscopic invariant features vector,  $I_{d_{(r_x, r_y)}}$  is the out-of-plane DRR at the  $r_x, r_y$  locations, and  $(i, j)$  are the image pixel coordinates. The maximum is found by exhaustive search on the 2D grid. Sub-grid accuracy is obtained by parabolic fitting and maximum extraction.

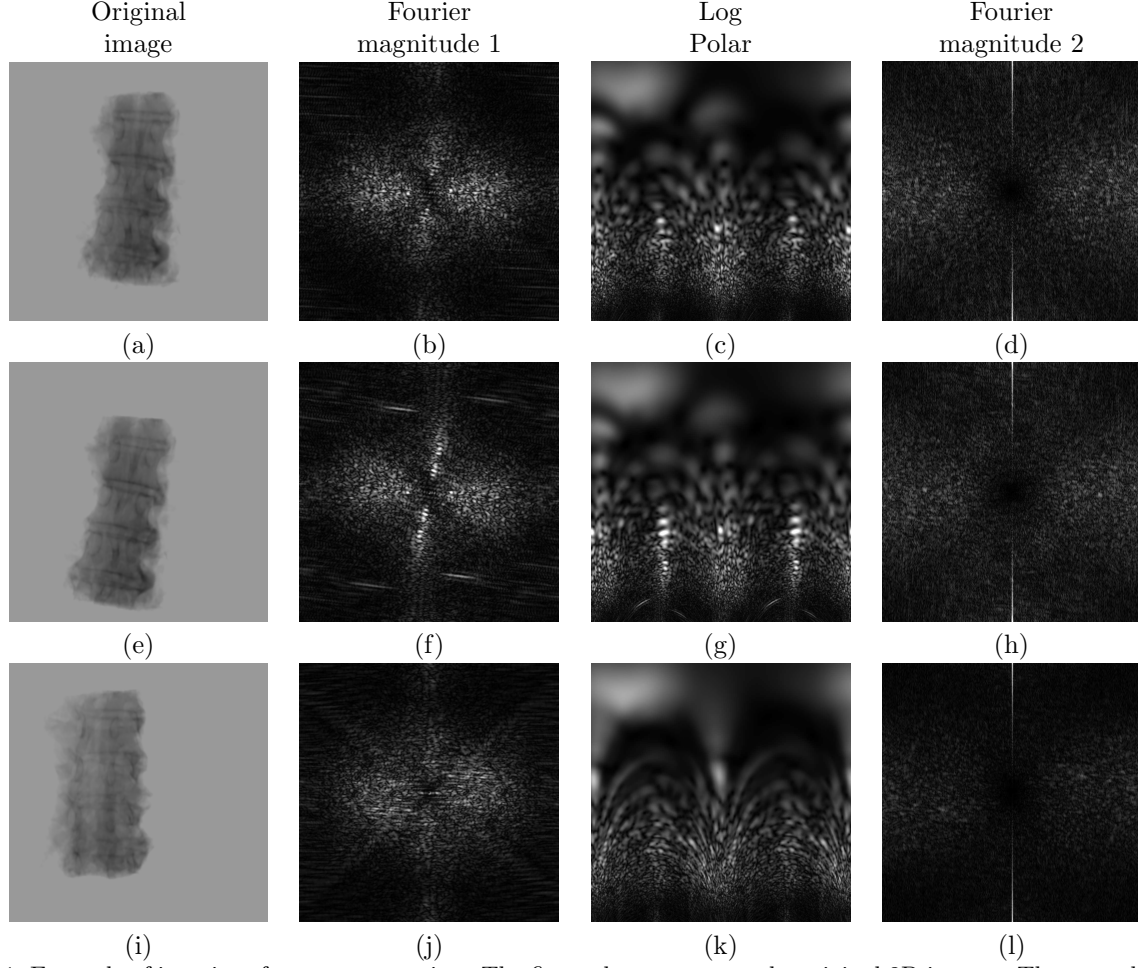


Figure 1. Example of invariant features generation. The first column presents the original 2D images. The second column presents the magnitude of the Fourier transform of each image. The third column the if Fourier transform magnitude in log-polar coordinates. The fourth column is the magnitude of the fourier transform of third column images. Note that the in-plane transformed image (e) does not affect the shape of its final Fourier magnitude (h), since it is invariant to in-plane transformations, while the out-of-plane transformed image (i) does affect the final shape of its Fourier magnitude (l).

## 2.4 In-plane parameters extraction

The in-plane parameters are computed by performing 2D/2D rigid registration with the Fourier-Mellin method. The method requires the computation of two FFTs, one image transformation into the log-polar domain, and two phase correlations.<sup>15</sup>

Let  $F_1(\xi, \eta)$  and  $F_2(\xi, \eta)$  be the Fourier transforms of images  $f_1(x, y)$  and  $f_2(x, y)$  respectively. When  $f_2$  differs from  $f_1$  only by a translation  $(x_0, y_0)$  (Eq. 1), their Fourier transforms are related by a phase difference:

$$F_2(\xi, \eta) = e^{-j2\pi(\xi x_0 + \eta y_0)} \cdot F_1(\xi, \eta) \quad (9)$$

The cross-power spectrum between the images is then defined as:

$$C(\xi, \eta) = \frac{F_1(\xi, \eta)F_2^*(\xi, \eta)}{|F_1(\xi, \eta)F_2(\xi, \eta)|} = e^{j2\pi(\xi x_0 + \eta y_0)} \quad (10)$$

where  $F^*$  is the complex conjugate of  $F$ . The Fourier shift theorem guarantees that the phase of the cross-power

spectrum is equal to the phase difference between the images. The inverse Fourier transform of Eq. 10 is:

$$c(x, y) = \delta(x - x_0, y - y_0) \quad (11)$$

which is approximately zero everywhere except at the optimal registration location.

The scale and the in-plane rotation parameters are obtained by applying the phase-correlation (Eq. 10) method on the log-polar representation of the magnitudes of the Fourier transform of the original images (Eq. 7). The translations are then obtained by applying the same method on the inverse rotated and scaled version of the image. The final transformation parameters are computed by averaging the parameters values from each fluoroscopic image.

### 3. EXPERIMENTAL RESULTS

We implemented our registration method in MATLAB<sup>®</sup>. We used clinical spinal CT and fluoroscopic images from the Van De Kraats et al. database.<sup>17</sup> This dataset also includes ground-truth transformations obtained with an additional 3D volume acquired intraoperatively with a 3D X-ray imaging system and an optical real-time tracking system.

The transformation between the fluoroscopic C-arm imaging device and the 3D X-ray system was computed with an the 3D/3D transformation between the preoperative CT and intraoperative 3D X-rays computed using high accuracy intensity-based registration algorithm. The final transformation between the CT and the fluoroscopic images served as the ground-truth.

To quantify the registration accuracy, we selected nine clinically relevant targets on the CT images. A total of 35 initial guess transformations were randomly generated in the  $\pm 10^\circ$  range for each rotation axis and  $\pm 15\text{mm}$  range for each translation axis. For each registration result, we measured both the error in the out-of-plane parameters estimation with respect to the initial estimation and the average final Target Registration Error (fTRE) with respect to the initial Target Registration Error (iTRE). The error in the estimation of two out-of-plane parameters was less than  $1.5^\circ$ , including large rotations, and required less than 1sec on A 3Ghz PC machine for each registration. The iTRE range was  $\pm 35\text{mm}$ . The fTRE range for iTRE range of  $\pm 18\text{mm}$  was less than  $\pm 4\text{mm}$ . Figure 2 shows an example of the registration results. Figure 3 describes the fTRE with respect to the sTRE. The mean running time of the entire registration was 9.5 sec (std=0.25secs).

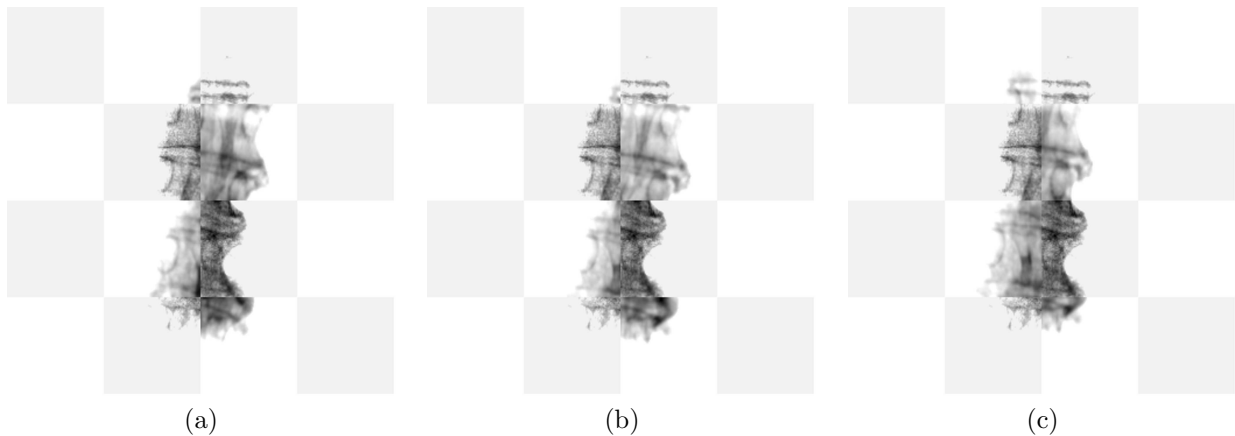


Figure 2. Example of the registration results, using combination of reference fluoroscopic image and generated DRR (in the gray regions): (a) before registration; (b) after out-of-plane registration, and; (c) after entire registration.

These results suggest that our algorithm is an effective method for fast and accurate estimation of the out-of-plane parameters, or for fast coarse registration with a wide convergence range. The resulting transformations can then be further refined by using them as the initial guess for fine intensity-based registration.

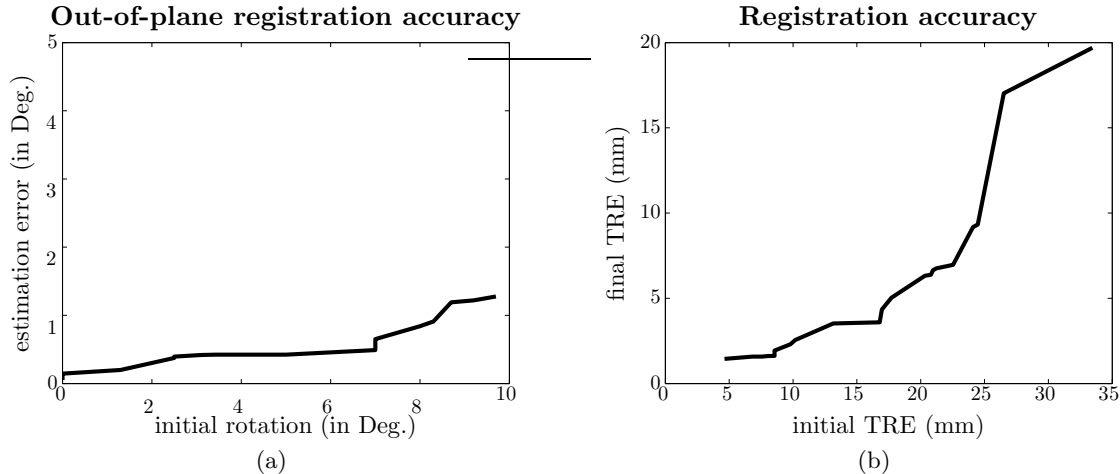


Figure 3. Registration results: (a) out-of-plane parameters estimation accuracy with respect to the initial out-of-plane offset; (b) overall registration accuracy – the final TRE is measured with respect to the initial TRE.

#### 4. CONCLUSION

We have presented a spectral-based method for the rigid registration of 2D X-ray images to a 3D CT image. Our method uses the Fourier representation properties to decompose the 6-dimensional problem into two decoupled two dimensional out-of-plane and four-dimensional in-plane problems. The 2D out-of-plane parameters are computed by maximization of the cross-correlation between the in-plane invariant features. The in-plane parameters are computed using a phase-correlation based method. Experimental results show that our algorithm is robust and fast compared to reported results of other intensity-based 2D/3D registration algorithm.

#### ACKNOWLEDGMENTS

Moti Freiman is partially supported by the Hebrew University Hoffman academic and social leadership program scholarship.

#### REFERENCES

- [1] Markelj, P., Tomazevic, D., Likar, B., and Pernus, F., “A review of 3D/2D registration methods for image-guided interventions,” *Med. Image Anal. In Press, Corrected Proof* (2010).
- [2] Markelj, P. et al, “Robust Gradient-Based 3D/2D Registration of CT and MR to X-Ray Images,” *IEEE Trans. Med. Imaging* **27**(12), 1704–1714 (2008).
- [3] Livyatan, H., Yaniv, Z., and Joskowicz, L., “Gradient-based 2D/3D rigid registration of fluoroscopic X-ray to CT,” *IEEE Trans. Med. Imaging* **22**(11), 1395–1406 (2003).
- [4] Groher, M. et al, “New CTA Protocol and 2D-3D Registration Method for Liver Catheterization,” in [*MICCAI’06*], *LNCS* **4190**, 873–881 (2006).
- [5] Zollei, L. et al, “2D-3D Rigid Registration of X-Ray Fluoroscopy and CT Images Using Mutual Information and Sparsely Sampled Histogram Estimators,” in [*IEEE CVPR’01*], 696–703 (2001).
- [6] Knaan, D. and Joskowicz, L., “Effective Intensity-Based 2D/3D Rigid Registration between Fluoroscopic X-Ray and CT,” in [*MICCAI’03*], *LNCS* **2878**, 351–358 (2003).
- [7] Khamene, A. et al, “Automatic registration of portal images and volumetric CT for patient positioning in radiation therapy,” *Med. Image Anal.* **10**(1), 96–112 (2006).
- [8] McLaughlin, R.A. et al, “A Comparison of 2D-3D Intensity-Based Registration and Feature-Based Registration for Neurointerventions,” in [*MICCAI’02*], *LNCS* **2489**, 517–524 (2002).
- [9] Russakoff, D.B. et al, “Fast generation of digitally reconstructed radiographs using attenuation fields with application to 2D-3D image registration,” *IEEE Trans. Med. Imaging* **24**(11), 1441–1454 (2005).

- [10] Russakoff, D.B. et al, "Intensity-based 2D-3D spine image registration incorporating a single fiducial marker," *Acad. Radiology* **12**(1), 37–50 (2005).
- [11] Tomazevic, D., Likar, B., and Pernus, F., "3D/2D registration by integrating 2D information in 3D," *IEEE Trans. Med. Imaging* **25**(1), 17–27 (2006).
- [12] Cyr, C.M. et al, "2D-3D registration based on shape matching," *IEEE MMBIA'00*, 198–203 (2000).
- [13] Fu, D. and Kuduvalli, G., "A fast, accurate, and automatic 2D-3D image registration for image-guided cranial radiosurgery," *Med. Phys.* **35**(5), 2180–2194 (2008).
- [14] Dong, S. et al, "The Zernike Expansion - An Example of a Merit Function for 2D/3D Registration Based on Orthogonal Functions," in [*MICCAI'08*], *LNCS* **5242**, 964–971 (2008).
- [15] Reddy, B. and Chatterji, B., "An FFT-based technique for translation, rotation, and scale-invariant image registration," *IEEE Trans. Image Proc.* **5**(8), 1266–1271 (1996).
- [16] Huy, T. and Goecke, R., "Optical flow estimation using fourier mellin transform," *IEEE CVPR'2008.*, 1–8 (June 2008).
- [17] Van De Kraats, E.B. et al, "Standardized Evaluation Methodology for 2D-3D Registration," *IEEE Trans. Med. Imaging* **24**(9), 1177–1190 (2005). <http://www.isi.uu.nl/Research/Databases/GS/>.